

Satellite system around the spiral galaxy NGC 5965

Laurent Nottale[1] and Pierre Chamaraux[2]

[1] LUTH, UMR CNRS 8102, Paris Observatory, 92195 Meudon CEDEX, France
e-mail: laurent.nottale@obspm.fr
[2] GEPI, UMR CNRS 8111, Paris Observatory, 92195 Meudon CEDEX, France
e-mail: pierre.chamaraux@obspm.fr

Received <date> / Accepted <date>

ABSTRACT

Aims. We have constituted a catalog of isolated giant galaxies surrounded by dwarf galaxies. From that catalog we have chosen to study the system of NGC 5965 and its fourteen companion galaxies.
Methods. We have analysed the structure of the NGC 5965 system and its internal motions by a new statistical deprojection method using pairs of satellites, which allows us to identify a disk structure despite the absence of 3 among 6 phase-space coordinates and to obtain a statistical measurement of its thickness. This method is validated using numerical simulations.
Results. We find that eleven among the companion galaxies are, with a high probability, bound satellites lying in a disk-like structure of radius 1 Mpc and thickness 0.14 ± 0.06 Mpc, two are unbound or out of plane and one is probably an interloper at cosmological distance.
Conclusions. We have found evidence that NGC 5965, a ($\approx$ 50 Mpc) distant galaxy, is surrounded by a low thickness disk-like system of satellites whose rotation velocity is constant up to about 200 kpc, then decreases beyond according to a Kepler law, up to 1 Mpc from the main galaxy.

Key words. Catalogs – Galaxies : groups : general

1. Introduction

We are engaged in a study of extragalactic multiple systems in order to better understand their dynamics (including determination of masses, M/L ratios, velocity PDFs, etc.). We have first constituted a Catalog of $\approx$ 13000 Isolated Pairs of Galaxies (Chamaraux & Nottale 2016, Nottale & Chamaraux 2018b) and we have derived their characteristic properties thanks to the use of new methods of statistical deprojection of inter-velocities and inter-distances between the pair members (Nottale & Chamaraux 2018a, Nottale & Chamaraux 2020).

Then we have considered the construction of an Isolated Galaxy Satellite Catalog (IGSC), where satellites (most of them being dwarf galaxies) are searched up to a projected distance of 1 Mpc from the main galaxy. Such central body gravitational systems are particularly interesting since they are the extragalactic equivalents of planetary systems, but at scales $\approx 10^{11}$ times larger. They could allow to test gravitation laws much farther than standard objects usually taken for scanning galaxy halos (stars, gas, globular clusters, etc.), which do not usually exceed distances of $\approx$ 50 kpc (except for our Galaxy and M31 where measurements reach $\sim$ 200 kpc (Bhattacharjee et al. 2014, Dai et al. 2022). In particular it could allow us to identify possible flattened structures at very large scales around isolated giant galaxies.

The existence of planes of satellite galaxies has been first suggested in our Local Group, around the Milky Way (Lynden-Bell 1976, Kunkel & Demers 1976) and M31 (Koch & Grebel 2006, McConnachie & Irwin 2006). Moreover the satellites of our Galaxy have also been found to co-orbit within their plane (Metz et al. 2008), achieving what has been called the Vast Polar Structure (VPOS). As regards M31, two different planar sub-systems have been identified, one with 13 co-rotational dwarfs (Ibata et al. 2013) and the other with 39 satellites (Santos-Santos et al. 2020).

A flattened structure has been discovered around the giant galaxy Cen A, made either of two thin planes (Tully et al. 2015) or one thick plane (Müller et al.

2019). Moreover, 21 out of the 28 dwarfs are found to be co-orbiting (Müller et al. 2021). The nearby galaxies M83 (Müller et al. 2018) and M101 (Müller et al. 2017, Anand et al. 2018) are also potentially surrounded by satellite planes.

A thin plane of 9 dwarf galaxies has been found around the galaxy NGC 253 in the Sculptor group (Martinez-Delgado et al. 2021), for which co-rotation is also probable, according to the known radial velocities.

Another interesting system has been found around the more distant galaxy NGC 2750 (≈ 40 Mpc) (Paudel et al. 2021), with six possible co-orbiting satellites, but in a not- flattened structure.

Finally, a statistical study (Heesters et al. 2021) of the MATLAS survey (Duc et al. 2015) (which has discovered ≈ 2000 dwarf galaxies around ≈ 200 early-type galaxies) has been used to systematically measure the flattening of the satellite systems. Heesters et al. found that around 30% of their satellite systems exhibit a significant flattening, more than what is expected from random distributions.

The question of the existence of planar structures among satellites of giant galaxies (Gottesman et al.1983, Zaritsky et al.1993, Carignan et al. 1997, Prada et al. 2003, Smith & Martinez 2003, Guttierez & Azzaro 2004, Müller & Jerjen 2020) is more and more discussed, since it constitutes, in addition to the 'Missing Satellite Problem' (Kauffmann et al. 1993, Klypin et al. 1999, Moore et al. 1999, Bullock 2010) a new fundamental puzzle for galaxy formation, the so-called 'plane of satellites problem' [PSP] (Pawlowski 2018). As emphasized by Müller (2023), "The plane of satellites problem is one of the most outstanding and heavily debated problems in near-field cosmology. It describes a discrepancy between the observed and predicted arrangement and motion of dwarf galaxy systems. In observations, dwarf galaxy systems around their host galaxies seem to be flattened and co-moving, while a more isotropic distribution and random motions is found in cosmological simulations" (in particular in the framework of the ΛCDM galaxy formation model).

With the aim to study these questions in the large scale environment of giant galaxies, we have searched in the HyperLeda database isolated galaxies of absolute magnitudes $M_G < -18.5$ and of radial velocities in the range V_G = 1000 km/s to 11500 km/s (distances from ≈ 15 to 160 Mpc). Our isolation criterion is the absence of any important galaxy within a radius of 1 Mpc around the main galaxy and within a velocity difference of 500 km/s (i.e. cosmological distance >≈ 7 Mpc for H_0 = 70 km/s.Mpc). We have therefore searched for satellite galaxies, defining them to have $M_S > M_G + 2.5$, a projected distance to the main galaxy < 1 Mpc and velocity difference $|\delta V| < 500$ km/s.

Then we have specifically analysed the galaxy systems having the largest number of satellites in an individual way in order to possibly find new examples of planar satellite distribution. In this study we found such an example with the system of NGC 5965 (an edge-on giant galaxy of absolute magnitude −22.1 and radial velocity 3383 km/s surrounded by 14 satellites with measured velocities), which we study in the present paper. The catalog and the statistical analysis of its data will be published in a future work.

In the present paper, first we describe the constitution of the IGSC (Section 1); then we present the satellite system around the giant spiral galaxy NGC 5965 (Section 2); we study in Section 3 its structure in projection on the sky, which suggests the existence of a common plane, and we compare its orientation to the plane of the main galaxy and to that of the Local SuperCluster (LSC). Then in Section 4, we deproject the distances of satellites to the main galaxy and we derive the deprojected inter-velocities. In Section 5, we develop new methods of analysis of the coplanarity of positions and velocities of couples of satellites, knowing that only 3 phase-space coordinates are available (X, Y and V_Z) instead of 6. We obtain a high probability for the existence of a common plane for 11 of the satellites. Then we study the distance-velocity relation in Section 6 under the perfect plane approximation, and we compare it to three models: the Navarro-Frenk-White ΛCDM model, the MOND model and a third model which combines a rotation at constant velocity (equal to the main galaxy flat rotation curve) for distances smaller than about 200 kpc and a Kepler law beyond, up to about 1 Mpc. We perform numerical simulations in Section 7, which validate the method, but also provides us with a statistical measurement of the disk thickness. We consider in Section 8 an extension of the environment of NGC 5965. These results are discussed in Section 9 and we conclude in Section 10.

2. Constitution of the IGSC

The Isolated Galaxy Satellite Catalog has been built by searching in the HyperLeda database 15 in the radial velocity range {1000, 11500} km/s for:

(i) main galaxies with B-band absolute magnitudes $M_G < -18.5$;

(ii) no other galaxy within a projected distance $r_p < 1$ Mpc, a radial velocity difference $|\Delta V| < 500$ km/s and an absolute magnitude difference $\delta M < 2.5$;

(iii) satellite galaxies defined by absolute magnitudes $M_s > M_G + 2.5$ and lying within $r_p < 1$ Mpc and $|\Delta V| < 500$ km/s from the parent galaxy. This means that the satellites have been chosen in such a way that their masses are at least 10 times smaller than the main galaxy mass, so that these systems are expected to achieve gravitational systems dominated by a central body (to some extent equivalent to planetary systems but at far larger scales).

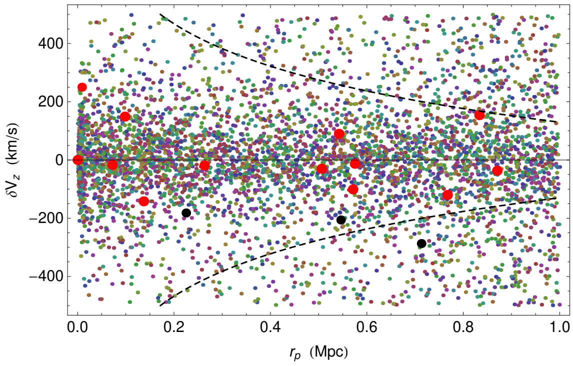

Fig. 1. Distribution of the (r_p, δV_z) values (where r_p is the projected interdistance between the main galaxy and a satellite on the sky plane, and δV_z is their radial intervelocity) for the satellites of NGC 5965 (red points). They are compared to the same distribution for the whole Isolated Galaxy Satellite Catalog (small points). The red point at $r_p = 0$ and $\delta V_z = 250$ km/s corresponds to an HyperLeda object which was initially in the satellite list, but which has been excluded as a satellite since its projected position lies inside the main galaxy. Its recorded velocity is in complete agreement with the NGC 5965 observed rotation curve at this distance from the center 20, so that it is probably just an inner part of NGC 5965. The dashed black curves show the expected cosmological limit: namely, galaxies beyond these curves have a high probability to not be satellites, but instead projected foreground or background interlopers. For this system, one expects only one false satellite, while there is just one object beyond the cosmological limit (object Nbr 12, black point). Two other objects (objects Nbr 5 and 9, black points) are found to be discrepant with the other satellites and could be gravitationally unbound to NGC 5965 or off-plane (see text).

3. Satellite system around NGC 5965

In the course of a first analysis of our catalog, we have searched for almost edge-on main galaxies (inclinations > 70 deg) surrounded by more than 10 satellites. Our aim was to possibly identify planar structures and to compare them to the host galaxy plane. Such a study would come in addition to the previous studies of our Galaxy, M31, Centaurus A and NGC 2750 as recalled in the Introduction, but reaching a larger scale for the satellite system (up to a diameter of 2 Mpc, of the order of magnitude of clusters of galaxies).

Among the large systems of our Catalog, NGC 5965 stands out as one of the best candidates, with an inclination of 90 deg and a clearly elongated projected structure of 14 satellites. It is one of the most luminous main galaxy of the catalog (absolute magnitude $M = -22.11 \pm 0.32$, blue band, HyperLeda data base) and has one of the largest number of satellites. Its rotation curve has been measured by Kuijken and Merrifield (1995). Its maximum rotation velocity (V_{rot}(gas) = 291 ± 10 km/s and V_{rot}(stars) = 220±50 km/s) confirms its status of giant spiral galaxy. The **potential** satellites have absolute magnitudes ranging from $M_6 = -19.3$ (corresponding to a mass 13 times smaller than the main galaxy mass) to $M_9 = -14.4$.

The distance to NGC 5965 is $d = 48$ Mpc acccording to its radial velocity $V = 3383$ km/s and taking $H_0 = 70$ km/s.Mpc. It agrees with that derived from distance indicators $d = (46 \pm 6)$ Mpc 37. The radius corresponding to the D_{25} angular diameter is $R_{25} = 36.0$ kpc for an adopted distance $d = 48$ Mpc.

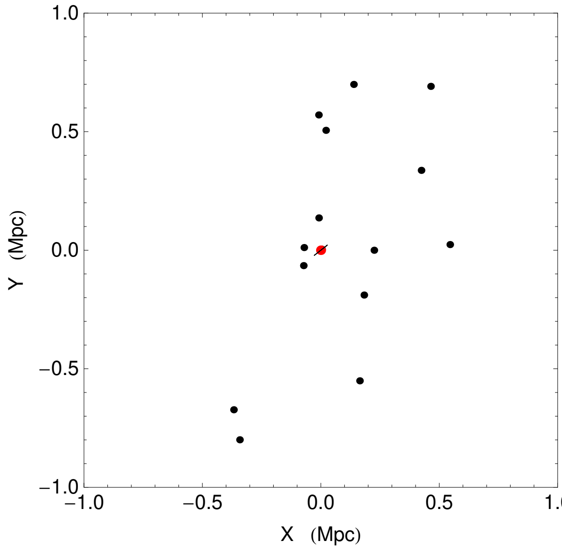

Fig. 2. Projection on the sky plane of the satellite positions in Mpc relative to the NGC 5965 (central red point), derived from the angular coordinates by taking a N5965 distance to the Sun of 48 Mpc. The small bar indicates the position angle of the main galaxy plane.

The list of the NGC 5965 satellites is shown in Table 1, which gives:(1) N^o, (2) name, (3) α_{2000} coordinate in decimal hour, (4) δ_{2000} coordinate in decimal degree, (5) apparent blue magnitude b_t, (6) absolute blue magnitude M_{abs}, (7) heliocentric radial velocity V_Z (km/s), (8) uncertainty on radial velocity σV (km/s).

Our basic data for the study of this satellite system consists of: (i) the position differences projected on the sky δx, δy between the potential satellites and the main galaxy, computed using a distance of 48 Mpc for NGC5965; (ii) their radial velocity differences δV_z . We combine δx and δy in terms of the projected interdistance $r_p = (\delta_x^2 + \delta y^2)^{1/2}$. We plot in Fig. 1 the (r_p, δV_z) distribution of the NGC 5965 satellites compared to the whole catalog distribution.

We have transformed the α, δ coordinates into true projected interdistances (in Mpc). The values of these interdistances and of the velocity differences with NGC 5965, X, Y and V_Z, are given in Table 2. The resulting observed positions are plotted in Fig. 2. The satellite distribution is clearly very elongated along an orientation with a position angle which we estimate to be 20 deg. This strongly suggests that the satellite system is a projected flattened disc-like structure. We shall analyse this hypothesis and support it hereafter with other arguments. It is also remarkable that NGC 5965 (which is edge-on with a position angle of 52 deg) is near to be parallel to the supergalactic plane (p.a.= 26 deg), and its orientation (p.a. = 63 deg) is also close to the projection axis of this disc-like satellite system (see Fig. 3).

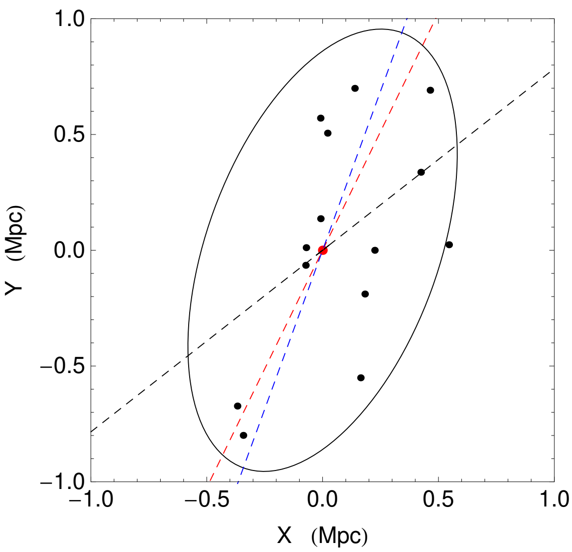

Fig. 3. Projection on the sky plane of the satellite system of NGC 5965 (red center point) in which we have drawn an ellipse (as a projected circle) suggesting a flat disk structure. We have also plotted the orientation axis of the edge-on main galaxy (black dashed line), the major axis of the ellipse which actually yields the projection angle of the satellite system (blue dashed line) and the local orientation of the supergalactic plane (red dashed line).

4. Rough deprojection of the satellite system

In order to deproject the possible disk structure of the satellite system, we have first made a more precise estimate of its position angle. In this purpose we have calculated the standard deviations of satellite positions along two orthogonal rotated directions and have optimized their ratio. We have found a position angle 70.2 deg for the major axis (in good agreement with our previous rough estimate), with largest elongation $\sigma_x = 0.49$ Mpc while $\sigma_y = 0.21$ Mpc yielding an axis ratio $\sigma_y/\sigma_x = 0.43$. Interpreted as the projection effect of a flat disk structure (see hereafter), this ratio would correspond to a projection angle $\phi = 64.6$ deg.

We have therefore performed a rotation of -70 deg on the sky plane by defining x and y along the principal axes. We show in Fig. 4 the result of this rotation, with a possible off-centering which symmetrizes the relative distribution of satellites (green point in Fig. 4. We have computed the center of gravity of the deprojected satellite system (excluding NGC 5965 and three objects which are not compatible with orbiting in the common plane, see hereafter), and we have found that it lies about half-way between the main galaxy and this apparent center of symmetry. This can be tentatively interpreted as an offset between the halo center (which would be traced by the satellite system) and NGC 5965 (a configuration possibly similar to the bullet cluster (Clowe et al. 2006), at exactly the same Mpc scale).

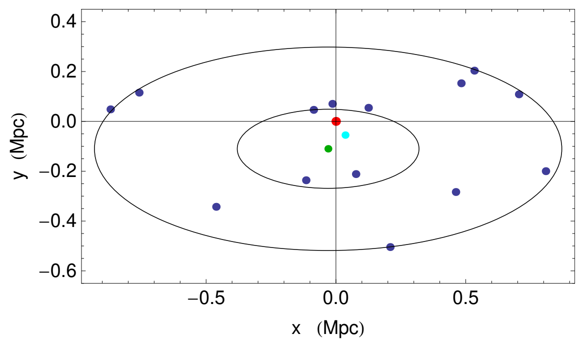

Fig. 4. Rotated view of the satellite system around NGC 5965 (red point) projected on the plane of the sky, with a possible off-centering (green point, center of symmetry of the satellite distribution), compared with the center of gravity of the satellite system (without NGC 5965, cyan point). In this representation, the satellites seem to be organized into two rings.

The anisotropy of the satellite distribution on the sky, clearly apparent in Fig. 4, suggests that it is the result of the projection of a disk-like structure with low thickness. We have estimated its projection angle to be $\phi = 64.6$ deg. The deprojected distribution is given

Table 1. List of data from HyperLEDA database for NGC 5965 and its possible satellites. Object N° 1 is the main galaxy, objects N° 2 to 15 are the potential satellites. Objects N° 5, 9 and 12 are found to be probable interlopers (see text). The coordinates are the *J*2000 right ascension and declination. The velocities are heliocentric radial velocities.

N°	Name	α (hour)	δ (deg.)	b_t	M_{abs}	V_r (km/s)	σ_V
1	NGC5965	15.56730	56.68578	12.69	-22.10	3383	10
2	PGC2544936	15.55712	56.69910	18.02	-15.68	3366	6
3	PGC214388	15.55682	56.60879	16.54	-17.25	3532	3
4	PGC2549587	15.56610	56.84736	16.61	-17.02	3241	4
5	PGC5064805	15.59968	56.68565	18.22	-15.33	3201	5
6	NGC5971	15.59358	56.46168	14.69	-19.31	3364	2
7	PGC055468	15.57038	57.28527	16.18	-18.02	3353	1
8	PGC3135837	15.62835	57.08513	17.46	-16.30	3473	2
9	PGC5064795	15.64579	56.71403	19.20	-14.39	3177	8
10	PGC055453	15.56601	57.36222	15.70	-18.41	3282	32
11	PGC055521	15.59095	56.03282	17.34	-16.35	3370	1
12	PGC2567028	15.58729	57.51478	16.31	-17.48	3096	1
13	PGC2517976	15.51439	55.88811	17.21	-16.44	3263	2
14	PGC2566856	15.63410	57.50509	17.68	-16.96	3537	2
15	PGC055286	15.51804	55.73799	15.94	-17.77	3346	2

in Fig. 5. However we find no corotation of this system: among the 11 galaxies identified as probable bound satellites (while galaxies N^o 5, 9 and 12 may be cosmological interlopers or unbound objects, see Appendix A), 7 are rotating in one direction and 4 in the other.

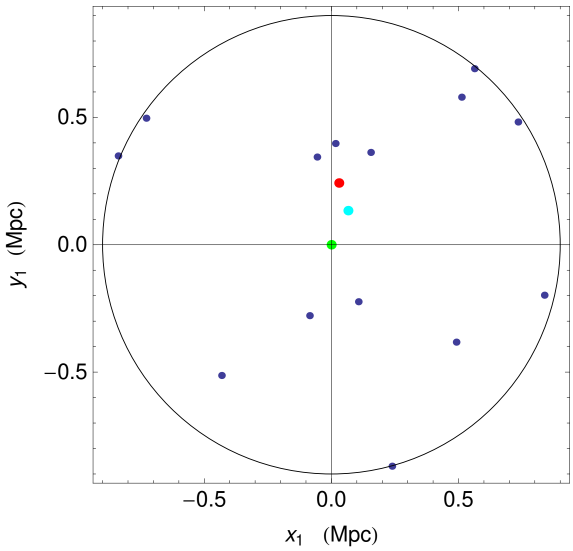

Fig. 5. Deprojected distribution of the satellite system around NGC 5965 (red point). The green point is an estimated center of symmetry of the system and the cyan point is its center of gravity (main galaxy and three objects excluded according to their dynamics, see text).

Table 2. Position (in Mpc) and radial velocity differences (in km/s) between the potential satellites and NGC 5965. Object N° 1A is projected on the visible part of NGC 5965 (object N° 1 in Table 1), at ≈ 6 kpc from its center and is probably just a luminous spot inside the galaxy. Its relative velocity, 251 km/s, agrees with the observed flat rotation curve of NGC 5965 (Kuijken & Merrifield 1995).

N°	Name	X	Y	V_Z
1A	PGC4118588	0.00438	0.00411	251
2	PGC2544936	-0.0707	0.0112	-17
3	PGC214388	-0.0728	-0.0649	149
4	PGC2549587	-0.0083	0.1363	-142
5	PGC5064805	0.2250	-0.00011	-182
6	NGC5971	0.1826	-0.1890	-19
7	PGC055468	0.0214	0.5057	-30
8	PGC3135837	0.4242	0.3368	90
9	PGC5064795	0.5454	0.0238	-206
10	PGC055453	-0.0090	0.5706	-101
11	PGC055521	0.1643	-0.5508	-13
12	PGC2567028	0.1389	0.6993	-287
13	PGC2517976	-0.3677	-0.6728	-120
14	PGC2566856	0.4642	0.6911	154
15	PGC055286	-0.3423	-0.7995	-37

5. Test of the law of dynamics at large distances

5.1. Statement of the problem

Up to now, the rotation curves of giant spiral galaxies have been observationally established from velocity measurements of stars, gas, globular clusters or dwarf companion galaxies, etc. Most of the time, these measurements are performed at distances from the center of the spiral galaxy which do not exceed ≈ 50 to 100 kpc see (Sofue 2016, Sofue 2018). They have yielded flat rotation curves which do not decrease up to such distances. These flat rotation curves are usually interpreted as the manifestation of a halo composed of dark matter. As remarked by (Sofue 2016) , " it is still difficult to obtain rotation curves in most of observed galaxies beyond 30 – 50 kpc. Thus, the measurements of the dynamical mass of dark halos in most galaxies are limited to radii of ≈ 20 – 30 kpc, where it is difficult to discriminate the halo models. Measurements at larger radii, up to ≈ 100 kpc, for a greater number of galaxies are crucial for conclusive comparison with the cosmological scenarios of structural formation".

Only the Milky Way and M31 rotation curves are known to far larger distances, but it is an interacting double system in which the halos seem to have merged.

Therefore our Isolated Galaxy Satellite Catalog provides us with a unique opportunity to study dynamics around isolated giant galaxies up to far larger distances (up to 1 Mpc).

This allows us to consider an important open question about this dynamics: do halos stop ? If they do, new questions occur: at which distance, and what happens beyond the halo end ? Under the hypothesis according to which the halos are made of (dark) matter, one expects to find again Kepler's law beyond the halo limit (if it exists).

Actually a strictly flat rotation curve would correspond to a halo density $\rho \sim r^{-2}$ and to a mass linearly increasing with distance, $M = M_0\, r/r_0$ which is therefore divergent. The Navarro-Frenk-White [NFW] model (Navarro, Frenk & White1996, Navarro, Frenk & White1997) has been empirically obtained from numerical simulations performed in the framework of the cold dark matter [ΛCDM] scenario. This model and the modified (Burkert 1995) model yields decreasing rotation curves and dark halo density profiles $\rho \sim r^{-3}$ at large scales, so that the mass is logarithmically increasing, $M \sim M_0 \ln(r/r_0)$ and therefore still divergent, even though more slowly. In the case when the number density of galaxies is large enough, the question of the limit of halos is not raised. However, in our case of strongly isolated galaxies, these two models require the existence of a cut-off, beyond which strict vacuum would be recovered, and therefore a Kepler rotation velocity law $\sim 1/\sqrt{r}$ or a faster decreasing density law. For example, r^{-4} and exponential halos yield a convergent mass.

We have the possibility to put these models to the test in the present work with the satellite system around the isolated giant galaxy NGC 5965, since it extends up to more than 1 Mpc (after deprojection), i.e. ≈ 20 times the previously available range for measuring rotation curves.

5.2. Main method: couples of satellites

Let (X, Y, Z) be the satellite coordinates in a 3D coordinate system centered on NGC 5965 and at its distance, where X is defined along the right ascension axis, Y declination in equatorial system and Z is the radial coordinate along the line of sight, all of them in Mpc (see Fig. 2). Let $(V_X,\ V_Y,\ V_Z)$ be their velocity differences with NGC 5965 in the same reference system, in km/s. The known variables are $(X,\ Y,\ V_Z)$, while $(Z,\ V_X,\ V_Y)$ are unknown.

We now define (x, y, z) and V_x, V_y, V_z in a coordinate system rotated by an angle θ around the line of sight (see Fig. 4):

$$x = X\cos\theta - Y\sin\theta, \quad y = X\sin\theta + Y\cos\theta. \tag{1}$$

Therefore $z = Z$ and $V_z = V_Z$. The repartition of the known and unknown variables remains the same in this coordinate system.

The (possible) satellite plane SP is assumed to be rotated by an angle ϕ around the x axis (see Figs. 4 and 5). Let us define the coordinates (X_p, Y_p) in this plane and Z_p orthogonal to the plane. They are related to the (x, y, z) coordinates by:

$$X_p = x,\ \ Y_p = y\cos\phi - z\sin\phi,\ \ Z_p = z\cos\phi + y\sin\phi. \tag{2}$$

5.2.1. One satellite

We shall use three conditions to be tested:

(i) The satellite lies in the plane SP. This is expressed by the equation:

$$z\cos\phi + y\sin\phi = Z_p = 0. \tag{3}$$

(ii) The satellite velocity lies in the same plane:

$$V_z\cos\phi + V_y\sin\phi = V_{Z_p} = 0. \tag{4}$$

(iii) The satellite orbit is nearly circular, so that the position and velocity vectors are orthogonal, i.e.

$$xV_x + yV_y + zV_z = 0. \tag{5}$$

When these three conditions are satisfied, the three unknown variables can be derived from the known ones and the SP plane rotation angle as:

$$V_x = \frac{y/x}{\cos\phi \sin\phi}\, V_z, \quad V_y = -\frac{V_z}{\tan\phi}, \quad z = -y \tan\phi. \quad (6)$$

The true 3D main galaxy-satellite distance and its relative velocity are now known:

$$R_0 = \sqrt{x^2 + \frac{y^2}{\cos^2\phi}}, \quad V_0 = |V_z/x|\, \frac{r}{\sin\phi}. \quad (7)$$

When the satellite lies in empty space beyond the host galaxy halo, these variables are related by the third Kepler's law,

$$GM(r) = r\, V^2 = \frac{V_z^2\, (y^2 + x^2 \cos^2\phi)^{3/2}}{x^2\, \sin^2\phi\, \cos^3\phi}, \quad (8)$$

in which $M(r)$ is the mass enclosed into the sphere of radius r. It is expressed here in terms of only the known variables and of the angle ϕ.

5.2.2. Two satellites

When all coordinates of position and velocity are known, the couple formed by the main galaxy and one satellite defines a plane. If one considers now a couple of satellites, the triangle they constitute with the main galaxy also defines a plane. But here this plane remains unknown since the radial coordinates z_1 and z_2 are unknown. However, the Kepler law allows one to identify a possible common plane for positions and velocities and to derive it from the six known variables, $(x,\ y,\ V_z)$ for both satellites. Namely in the vacuum case where GM =cst beyond the halo limit, one finds in the circular approximation:

$$GM = \frac{V_{z1}^2\, (y_1^2 + x_1^2 \cos^2\phi)^{3/2}}{x_1^2\, \sin^2\phi\, \cos^3\phi} = \frac{V_{z2}^2\, (y_2^2 + x_2^2 \cos^2\phi)^{3/2}}{x_2^2\, \sin^2\phi\, \cos^3\phi}. \quad (9)$$

One finds the following expression for the variable $T = \cos^2\phi$ from which the plane angle ϕ can be derived:

$$T = \frac{y_2^2\, (x_1^4\, V_{z2}^4)^{1/3} - y_1^2\, (x_2^4\, V_{z1}^4)^{1/3}}{x_1^2\, (x_2^4\, V_{z1}^4)^{1/3} - x_2^2\, (x_1^4\, V_{z2}^4)^{1/3}}. \quad (10)$$

Once the plane angle known from this equation, the mass of the host galaxy can be itself derived (although with a large uncertainty).

When the satellites lie inside the halo, a more complicated relation is still possible, but with different values of $GM(r)$ for the two satellites since they are a priori expected to lie at different distances r_1 and r_2 from the main galaxy. Therefore one obtains a similar expression for $\cos^2\phi$, in which V_{z1}^2 is replaced by $V_{z1}^2/M(r_1)$ and V_{z2}^2 by $V_{z2}^2/M(r_2)$, where $M(r)$ is given by the halo model.

To our knowledge, this is a new deprojection method where 6 coordinates from two satellites (4 positions and 2 velocities) can be combined to derive the plane in which they lie, instead of the standard 3D geometry without need of deprojection, where one uses 3 positions and 3 velocities for one satellite.

Thanks to these equations, we can now numerically verify that most satellites lie indeed in or close to a plane and determine the characteristics of this plane.

5.3. Application to the NGC 5965 system

We have calculated the parameter T as given in Eq. 10 for all couples of satellites. When a given satellite couple defines a well definite plane for a given main galaxy mass, the parameter $T = \cos^2\phi$ is therefore constrained to be $0 < T < 1$.

The number of couples which satisfy this constraint depends on the rotation angle θ on the sky plane. Therefore, by optimizing this number, one obtains a measure of θ. One finds $\theta = -69$ deg, in good agreement with our direct initial rough estimate 70 deg and its precise determination from the standard deviation ratio of positions, $\theta = -70.2$ deg.

5.3.1. High probability of the existence of a satellite plane

We find a maximal number of 33 available couples among 91 possible couples for 14 satellites. We have calculated the probability of obtaining such a result by chance by simulating random systems under the same conditions of distances and velocities as the real system: we have found $P = 0.0035$.

This result corresponds to a global computation on the whole range $T = 0 - 1$. However, as can be seen in Fig. 7, the distribution of $\cos\phi$ values clusters around small values of T, so that the statistical significance of the effect is actually higher. Indeed, one expects 13% of couples to lie by chance between $0 < T < 1$, i.e. 12 couples among 91 instead of 33 observed. Beyond $\cos\phi = 0.4$ we find 8 available couples, which is exactly the number expected by chance. As a result, for $\cos\phi < 0.4$, 25 are observed while only 4 are expected. The probability of such a result is found in the simulation to be only $P = 0.0017$.

Now three of the satellites, numbers 5, 9 and 12, are found to be unbound with NGC 5965 (see Appendix A and what follows), i.e to be false satellites, or at least not to contribute to the plane.

We are left with 11 true satellites, numbers 2, 3, 4, 6, 7, 8, 10, 11, 13, 14 and 15. With these eleven satellites we can make 55 couples. We find 28 of these couples that satisfy the constraint $0 < T < 1$. The probabiliy of obtaining such a result by chance is found to be $P = 0.00041$ (i.e., only 41 such cases among 100 000 have been obtained in the simulation).

Finally even this low probability of 4×10^{-4} overestimates the true probability. Indeed, the observed distribution of the T values shows 21 couples between 0 and 0.2 (while 1.4 are expected) and 7 between 0.2 and 1 which is close to the expected random value of 5.6. The probability to obtain by chance such a distribution is found by the simulation to be only $P = 3 \times 10^{-5}$. We have again calculated these probabilities by accounting for the (low) uncertainties on the velocity measurements (see Table 1), while the position errors can be considered negligible. This account does not change these conclusions.

We conclude that the existence of a bounded plane structure for the remaining system of eleven satellites is very highly probable. This result will be further supported by numerical simulations in the following Sec. 7.

5.3.2. Value of the plane angle

The mean value of T is $\langle T \rangle = 0.183 \pm 0.045$, corresponding to a predicted angle $\phi = (1.13 \pm 0.05)$ rd $= (64.7 \pm 2.9)$ deg. It is in excellent agreement with our previous rough estimate 63 deg based on the deprojection performed from Fig. 4 to Fig. 5 and with the more accurate determination from 2D standard deviations of the position distribution, which yielded $\phi = 64.6$ deg.

The mean value of ϕ is $\langle \phi \rangle = 1.18$ (68 deg). However the PDF of ϕ shows a narrow peak for $\phi = 1.246 \pm 0.004$ (71 deg) which contains 13 couples among 28, as can be seen in Fig. 6.

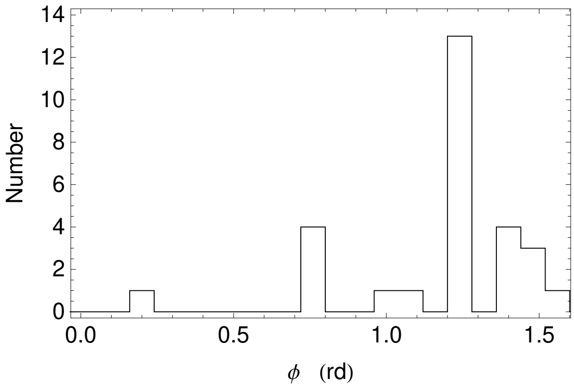

Fig. 6. Observed distribution of the values of ϕ derived from the 28 satellite couples which satisfy the relation $0 < T < 1$ (the 3 false satellites (5, 9, 12) being excluded).

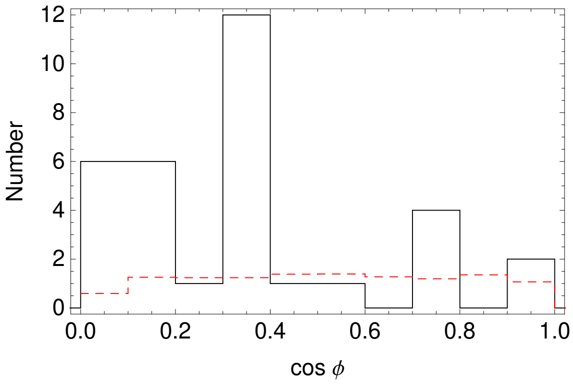

Fig. 7. Observed distribution of the absolute values of $\cos\phi$ derived from the 33 satellite couples which satisfy the relation $0 < T < 1$. The dashed red line is the random number expected from pure chance.

6. Distance-velocity relation for the satellite system: plane approximation

6.1. Best configuration for projection angle

The previous study has proved that 11 of the satellites are quite compatible with lying in a plane or close to a plane, while 3 of them (numbers 5, 9 and 12) are excluded. Satellite number 12 is compatible as being a projected foreground galaxy at a cosmological distance of ≈ 4 Mpc, since it lies into the cosmological domain (see Fig. 1), while the number of cosmological projected galaxies expected in the field of 1 Mpc radius around NGC 5965 is just 1. Objects 5 and 9 cannot be associated to the other satellites as forming a coherent system, and could either be unbound interlopers crossing the NGC 5965 system, or other satellites which are not included in the planar system.

From our knowledge of angles θ and ϕ, we can now calculate the true positions and velocities of the satellites under the hypothesis that they lie in a single plane and plot them in a (distance-velocity) diagram. According to our previous study, we have considered three possible values for ϕ. Whatever this value, we find that the satellite system can be decomposed into two well-separated populations, a near one ("N", $\approx 0.15 < r <\approx 0.20$ Mpc) and a far one ("F", $\approx 0.6 < r <\approx 1$ Mpc).

(1) $\phi = 1.13$: in this case, the mean distance and velocity of the near subsystem are: $r_N = (0.161 \pm 0.013)$ Mpc and $V_N = 232 \pm 14$ km/s. This points to a rota-

tion curve which remains flat up to 160 kpc. It yields a halo mass $GM_N(r) = r_N V_N^2 = 8600$ Mpc.(km/s)^2, which corresponds to $M/L = 32$ in solar units. For the distant subsystem one finds: $r_F = (0.779 \pm 0.048)$ Mpc and $V_F = 110 \pm 23$ km/s. The total mass inside 800 kpc has only slightly increased, $GM_N(r) = r_F V_F^2 = 9400$ Mpc.(km/s)^2, supporting the fact that the halo does not extend beyond ≈ 200 kpc.

(2) $\phi = 1.24$: in this case one finds: $r_N = (0.200 \pm 0.018)$ Mpc and $V_N = 275 \pm 12$ km/s. This value is larger than the measured rotation velocity in NGC 5965 (star rotation curve 220 km/s + one sub-region at ≈ 10 kpc measured at 250 km/s). It yields a halo mass $GM_N(r) = r_N V_N^2 = 15100$ Mpc.(km/s)^2 inside 200 kpc, which corresponds to $M/L = 59$ in solar units. For the distant subsystem one finds: $r_F = (0.896 \pm 0.055)$ Mpc and $V_F = 121 \pm 25$ km/s. The total mass inside 900 kpc has decreased, $GM_N(r) = r_F V_F^2 = 13100$ Mpc.(km/s)^2, which is impossible and leads therefore to reject this configuration.

(3) $\phi = 1.18$ (mean of ϕ). In this case (favoured) one finds: $r_N = (0.175 \pm 0.015)$ Mpc and $V_N = 246 \pm 13$ km/s, in full agreement with the rotation velocity measurements inside NGC 5965 and therefore supporting a constant rotation velocity up to 175 kpc. It yields a halo mass $GM_N(r) = r_N V_N^2 = 10500$ Mpc.(km/s)^2, which corresponds to $M/L = 41$ in solar units, i.e. about 7 times the luminous mass, therefore allowing this halo to be made of baryonic dark matter only, without need for non-baryonic dark matter at this level (the limit being ≈ 9 according to primordial nucleosynthesis). For the distant subsystem one finds: $r_F = (0.820 \pm 0.049)$ Mpc and $V_F = 113 \pm 23$ km/s. The total mass inside 800 kpc has remained the same, $GM(r) = r_F V_F^2 = 10500$ Mpc.(km/s)^2, supporting the fact that the halo does not extend beyond ≈ 175 kpc, that space is empty beyond this limit and that Kepler's law $V = \sqrt{GM/r}$ with M =cst is validated between distances of 175 kpc and more than 1 Mpc.

The velocity difference between the Near and Far sub-systems is $\Delta V = (133 \pm 26)$ km/s, statistically significant at the 5 σ level. To our knowledge, it is the first time that a velocity decrease is found around a galaxy with such a very high statistical significance and at such a large distance. This result has been anticipated by (Prada et al. 2003), but at smaller scales and with only a marginal significance. They have probed the halo mass distribution by studying the velocities of satellites orbiting isolated galaxies using the Sloan Digital Sky Survey (SDSS). They have found that the rms line-of-sight velocity differences between their primary galaxies and their satellites changes from 120 km/s at 20 kpc to 60 km/s at 350 kpc, with a statistical significance of this decline at the 97% level, thus corresponding to a marginal $\approx 2\sigma$ statistical significance.

The corresponding satellite values and their mean and standard deviations of the mean are shown in Fig. 9.

6.2. Comparison to theoretical models

We compare here the observed interdistance-intervelocity relation of the satellite system aroung NGC5965 with three theoretical models: Kepler's law (i.e. Newton's law in vacuum), Navarro-Frenck-White [NFW] halos, which result from numerical simulations in the ΛCDM model of structure formation (corresponding to a $\sim r^{-3}$ halo) and MOND (modification of Newtonian dynamics aimed at accounting for flat rotation curves of galaxies (Milgrom 1983)).

Another proposal for accounting for the anomalous dynamics observed beyond the galaxy luminous scales consists of attributing it to the fractality of spacetime (Nottale 2001, LeBohec 2022, Cresson, Nottale & Lehner 2021). This new geometry manifests itself in terms of a "dark potential" having the form of a quantum-like potential, in a way similar to curvature manifesting itself as the Newtonian potential in Einstein's gravitation theory. We shall not consider this approach here, but develop it further in a forthcoming work.

6.2.1. Kepler's law

As already remarked hereabove, our data and its deprojection is in good agreement with Kepler's law $V = \sqrt{GM/r}$, since we find a mass which has not been modified or very slightly changed between the Near subsystem at ≈ 175 kpc and the Far subsystem at ≈ 800 kpc. We have found a total mass $GM = r_N V_N^2 = r_F V_F^2 = 10500$ Mpc.(km/s)^2, which corresponds to $M = 2 \times 10^{12}$ $M_\odot$ and a mass to luminosity ratio $M/L = 40$. The deprojected distance-velocity relation obtained for this mass and under the assumption that the satellite lie in a perfect plane is plotted in Fig. 8.

This result supports the view that the halo does not extend beyond the Near subsystem and that the density vanishes or becomes negligible beyond this limit. This result may be questioned since it is obtained under the perfect plane approximation. However, we shall see in Sec. 7 that the satellite couple method can be used to obtain a direct measurement of the disk thickness, and that this measurement supports a low thickness (axis ratio $\approx 1/7$).

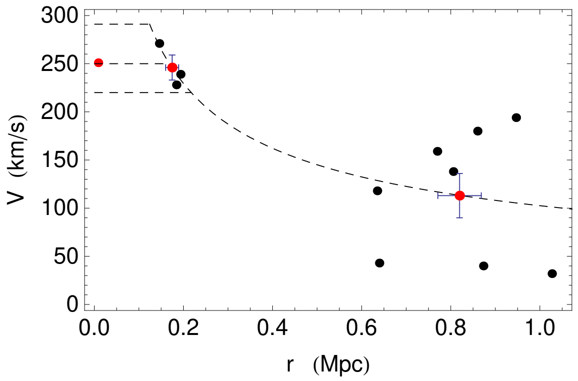

Fig. 8. Distance-velocity relation for the satellites of NGC 5965 under the plane disk approximation. The variables r and V are the 3D deprojected inter-distances and inter-velocities relative to the main galaxy. The deprojection is performed for a mass of NGC 5965 given by $GM = 10500$ Mpc.(km/s)^2 (corresponding to a ratio $M/L = 40$ in solar units) inside ≈ 175 kpc, under the assumption that the satellites lie in a perfect plane. The red points with error bars are the mean and the standard error of the mean for the two groups which are evidenced. The red point near the origin represents both the inner rotation curve of NGC 5965 and a velocity measurement for a 'satellite' lying at a relative distance 6 kpc which is most probably an inner part of the galaxy. It allows one to check that the rotation curve has remained constant up to ≈ 175 kpc. The decreasing dashed curve is the Kepler law $V = \sqrt{GM/r}$. The three horizontal dashed lines stand for various measurements of NGC5965 flat rotation curves for stars (lower value) and gas (upper value) (Kuijken & Merrifield 1995).

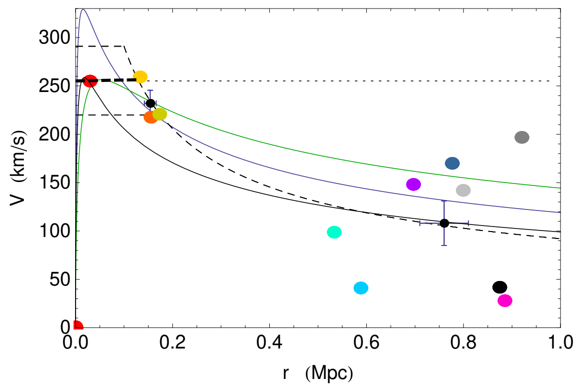

Fig. 9. Distance-velocity relation for the satellites of NGC 5965 compared with that expected from different models. Dashed curves: Kepler law. Dotted line: MOND model. Continuous curves: NFW model. The blue continuous curve is fitted to account at ±1 sigma for the Near and Far sub-systems. The green curve fits the center and the Near sub-system. The black curve fits the center and the far sub-system. The decreasing dashed curve is the corresponding Kepler law $V = \sqrt{GM/r}$ for an isothermal halo extending up to ≈ 180 kpc. The dashed constant lines stand for 3 values of the flat rotation velocity (stars, mean and gas).

6.2.2. NFW halo

The NFW halo (Navarro et al. 1996, Navarro et al. 1997) has been empirically obtained from numerical simulations in the scenario of cold dark matter galaxy formation. It also leads to a decrease of the velocity, but less steep than in the Kepler case. The halo density varies at large distances as $\approx r^{-3}$, so that the velocity varies as $V \sim \sqrt{\ln r/r}$. More precisely, the velocity is expected to vary as:

$$\frac{V_c(r)}{V_0} = \frac{r_0}{r}\,\frac{\ln(1 + c\,r/r_0) - (c\,r/r_0)/(1 + c\,r/r_0)}{\ln(1 + c) - c/(1 + c)}, \quad (11)$$

where r_0 is the virial radius. In this model, the circular velocity peaks at $r_{max} = 2r_0/c$. We have not found any possible fit by this model capable of accounting for the three known domains: (i) the observed flat rotation curve for $r < 35$ kpc with $V = 230$ km/s, possibly supplemented by a point at $V = 250$ km/s and $r = 6$ kpc (corresponding to an object which was initially in the satellite list but which we have identified with a part of NGC 5965); (ii) the Near subsystem at 150-200 kpc and $V \approx 250$ km/s; (iii) the Far subsystem at ≈ 800 kpc and $V \approx 110$ km/s. Fitting the velocity peak in NGC 5965 yields a strong disagreement with the satellites. An acceptable fit of the Near and Far subsystems is possible (Fig. 9), but it yields a sharp peak at 330 km/s or more which disagrees with the observed rotation curve (Kuijken & Merrifield 1995). The three continuous curves in Fig. 9 correspond to fitting two of the three sub-systems, but do not fit the third.

6.2.3. MOND

The essence of the MOND proposal is that Newton's law is no longer valid when accelerations become smaller than a critical acceleration which is estimated to be $a_0 = 1.2 \times 10^{-10}$ m/s^2. Therefore, any observation of a Newtonian regime for accelerations smaller than this value would invalidate the MOND model.

In a recent work, Dai et al (2022) have studied the rotation curves of our Galaxy and M31 out to large distances and weak accelerations. They find from numerical simulations that, in the ΛCDM model, the dark halos are saturated at very large distances and the acceleration then decreases as Kepler laws. They conclude that there are strong indications that the rotation curves deviate from the MOND prediction for accelerations below 10^{-11} m/s^2 and that, at very large distances, the data are easier to accommodate in the ΛCDM model than in the MOND model.

In the case of NGC 5965, the MOND critical value is obtained just inside the luminous radius of the galaxy, at $r = 35$ kpc. The rotation curve remains flat up to $\approx$ 175 kpc. At this distance, the acceleartion is $a_N = a_0/10 \approx 10^{-11}$ m/s^2, which could be accounted for by the MOND hypothesis without dark matter. However, the velocity decreases in a Keplerian way beyond this point, in contradiction with MOND prediction for still smaller accelerations (see Fig. 9). The acceleration reaches a very low value, 230 times smaller than the MOND limit, $a_F = a_0/230 = a_N/22$ in the distant satellite subsystem at $\approx$ 0.8 Mpc, thus invalidating the MOND model in this satellite system.

This result is obtained with only one galaxy and its satellites, but in works to come, we shall study this question with our whole IGSC catalog of giant isolated galaxies and their satellites.

7. Numerical simulations

7.1. The "Near" sub-system

The sub-system of 3 galaxies close to NGC 5965 (N^o 2, 3 and 4) deserves a specific treatment. Indeed the couple method gives remarkably coherent results for these 3 objects, as can be seen in Table 3. This is particularly striking in the concordant values of GM, knowing that its values obtained by our couple method tend to vary by an order of magnitude. One finds mean values $\langle T \rangle = \langle \cos^2 \phi \rangle = 0.107 \pm 0.007$ (error on the mean), $\langle \phi \rangle = 70.8 \pm 0.6$ deg and $\langle GM \rangle = 14000 \pm 800$ Mpc.(km/s)^2.

Table 3. Couples among the three galaxies in the "Near" sub-system. The value of $T = \cos^2 \phi$ is computed from the observed positions and velocities relative to NGC 5965 using Eq. 10 and GM using Eq. 9. The three couples yield remarkably consistent values of both the angle and main galaxy mass, implying that they lie in a thin disk with a high probability.

Couples	T	ϕ (rd)	GM [Mpc.(km/s)^2]
2, 3	0.1144	1.225	13179
2, 4	0.1116	1.230	13633
3, 4	0.0972	1.253	15392

We have estimated the probability to obtain such a result by chance by performing a numerical simulation in which x and y are taken at random between -1 and 1 Mpc while V_z is randomly chosen in the interval $(-300, 300)$ km/s. We find a probability $P = 0.013$ to obtain 3 couples with $0 \leq T \leq 1$, so that the probability for the 3 values to lie in an interval of width $0.017 \approx 2\sigma$ as observed can be estimated as $P = 2 \times 10^{-4}$. We conclude that this sub-system of 3 satellites and their velocities relative to NGC 5965 lie in a thin disk around the main galaxy with a high probability.

7.2. Numerical simulations of a thick disk: measurement of thickness by the couple method

In the case of a perfectly flat disk, one would expect all the satellite couples to yield exactly the same value of $T = \cos^2 \phi$. In the case of a thick disk, different values are expected while their distribution should be indicative of its thickness. One therefore could hope that the observed number of couples would actually yield a measurement of the disk thickness.

In order to study this possibility, we have first made numerical simulations of randomly distributed phase-space coordinates (X and Y between -1 and -1 Mpc and V_Z between -300 and $+300$ km/s for 11 companion galaxies). In each random realization we have computed the number of obtained couples with $0 < T < 1$, where T is given in Eq. 10. The result for 10000 realizations is given in Fig. 10. It yields the PDF of the number of expected couples in the no-disk case. One finds a peak for 5 couples while the mean is 6 couples. The number observed for the 11 satellites around NGC 5965, $N_c = 28$ couples, is confirmed to be highly unprobable in this random case ($P < 10^{-4}$).

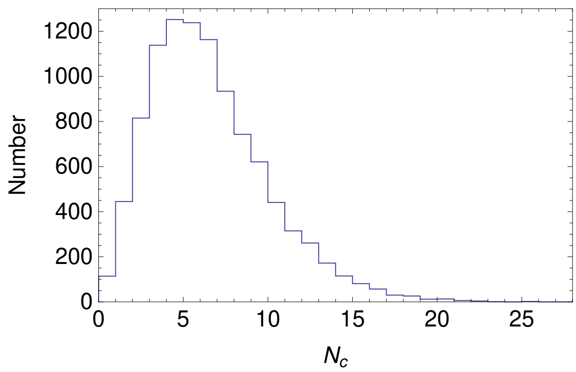

Fig. 10. PDF of the number of couples with $0 < T < 1$ expected for 11 randomly distributed companion galaxies (not lying in a disk). It clearly shows that the observed number of couples, $N_c = 28$, is highly unprobable in this case and therefore supports the existence of a disk.

Then we have performed another numerical simulation in which we have distributed 11 galaxies in a thick disk following a Gausssian distribution of standard deviation σ_{Z_p} in the plane coordinate Z_p orthogonal to the disk. Note that, owing to the small number of objects, the half-extension of the disk is close to σ_{Z_p} while its radius is ≈ 1 Mpc, so that its relative thickness will also be $\approx \sigma_{Z_p}$.

We have projected the space coordinates on the plane of the sky (and on the line of sight for velocities) with a projection angle $\phi = 1.18$ as obtained for the observed data. Then we have counted the number of couples with $0 < T < 1$ for various values of σ_{Z_p}. We have also added possible deviations of velocities from a pure plane by taking random values of V_{Z_p} in the range $(-V_0, V_0)$. We have performed 1000 random realisations for each value of σ_{Z_p} and V_0, from which the PDFs of the number of couples have been derived (and found to be close to Gaussian).

We give in Fig. 11 the mean and standard deviation of this PDF in function of the disk thickness σ_{Z_p}. Except for very thin disks, the effect of velocity deviations from a flat disk remains small (dashed curve). As hoped, this method yields a genuine measurement of the disk thickness including its uncertainty. We find that the observed value of 28 couples for 11 potential satellites corresponds to a disk with a low thickness $\sigma_{Z_p} = (0.14 \pm 0.06)$ Mpc. This result definitely proves that NGC 5965 is surrounded by a system of satellites distributed in a relatively thin disk.

This will now be checked and confirmed by another numerical simulation in which we keep the known coordinates and simulate the missing ones in a random way.

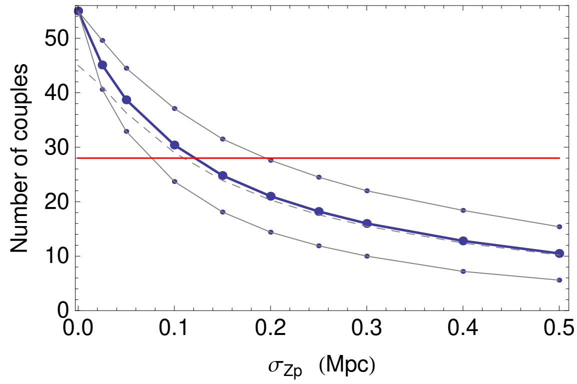

Fig. 11. Number of couples satisfying $0 < T < 1$ expected for 11 satellites distributed in a disk of thickness σ_{Z_p} (one sigma of a Gaussian distribution). The figure gives the mean and standard deviation of the PDF obtained in each case for 1000 random realizations. The dashed curve is the mean number of couples obtained when adding a random deviation of velocities from the mean plane in the range $(-30, +30)$ km/s. The red horizontal line is the number of couples observed for the 11 companion galaxies to NGC 5965 which have been identified as possible bound satellites. The number of couples obtained for a ramdom distribution, $N_c = 6$, is recovered as expected when one extrapolates this curve up to $\sigma_{Z_p} \approx 1$.

7.3. Numerical simulations of missing coordinates

The application of our test using couples of galaxies has yielded a high probability for the existence of a disk with low thickness. This result tends to indicate that, despite the absence of the 3 phase-space coordinates Z, V_X and V_Y, which may a priori take any value, the 3 remaining coordinates X, Y and V_Z nevertheless carry information about the potential disk and its thickness. This comes from the couples method, which allows to recover 6 phase-space coordinates by considering two companion galaxies and the plane that they form with the main galaxy (here NGC 5965).

In order to confirm these results, we have performed numerical simulations of the missing coordinates while keeping the observed values of the known ones. We have drawn at random 10000 configurations for 11 satellites such that $R = (X^2 + Y^2 + Z^2)^{1/2} < R_0$, with $R_0 = 1$ Mpc and $V = (V_X^2 + V_Y^2 + V_Z^2)^{1/2} < V_0$, with $V_0 = 300$ km/s. Then we have measured for each configuration the standard deviation of the disk thickness along the plane coordinate Z_p, keeping the values $\theta = -70$ deg$= -1.22$ rd and $\phi = 1.18$ rd which defines this plane from the known coordinates. The resulting PDF of the disk thickness is given in Fig. 12. It is very well fitted by a Gaussian distribution of mean 0.252 Mpc and dispersion 0.045 Mpc. This is to be compared with its X and Y extension reaching ≈ 2 Mpc. This is a remarkable result, since this means that one obtains a relatively thin disk in all cases, whatever the missing coordinates. A typical example of the aspect of the obtained mean configuration is given in Fig. 13.

The reconstructed configuration of Appendix A, in which we have given the possible missing coordinates allowing minimal Z_p values would correspond to the lowest dispersion in this simulation, $\sigma_{Z_p} \approx 0.1$. It also agrees with the range of possible values $(0.08 - 0.20)$ that we have obtained as corresponding to the observed number of couples, $N_c = 28$. A second example of reconstruction, in which we chose instead minimal possible values of the eccentricity of the satellite orbits, yields a standard deviation $\sigma_{Z_p} \approx 0.23$, close to the mean of the simulation. The measured thickness from the couple method, $\sigma_{Z_p} \approx 0.14 \pm 0.06$ lies between these two extreme configurations.

This proves that the known phase-space coordinates indeed contain information about the existence of a disk with moderate or low thickness, despite the absence of three coordinates among six.

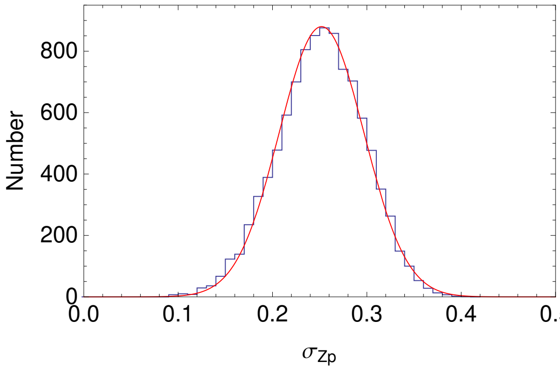

Fig. 12. PDF of the standard deviation of the disk thickness (in Mpc) obtained by keeping the known phase-space coordinates and randomly simulating the missing ones.

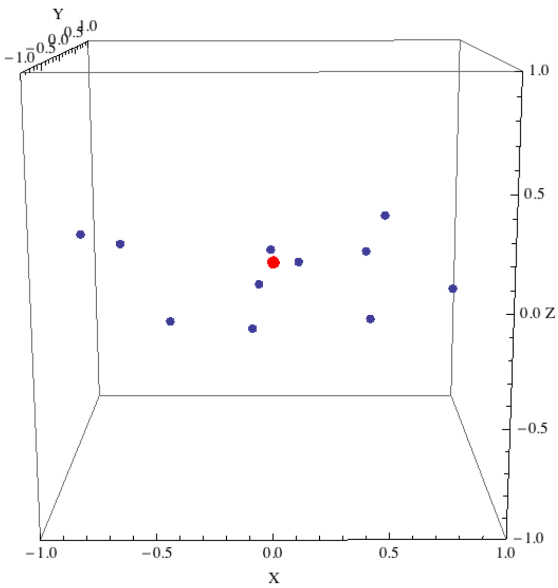

Fig. 13. Typical example of a disk obtained from keeping the known phase-space coordinates and taking at random the missing ones. In this example $\sigma_{Zp} = 0.25$ (corresponding to the mean standard deviation obtained in the simulation), larger than the value measured by the couple method, $\sigma_{Zp} = 0.14 \pm 0.06$.

7.4. Kepler law: simulation of missing coordinates in a thick disk

Finally we have reconsidered the question of a possible Kepler law for the satellite system. It has been obtained previously only under the hypothesis of a strictly flat disk, which we have found to be unprobable.

In order to overcome this limitation, we have performed simulations of the missing coordinates while keeping the known ones. We have taken the offset with respect to the mean plane Z_p at random in disks with Gaussian distribution of thickness $\sigma_{Z_p} = (0.14 \pm 0.06)$ Mpc (as measured by the couple method) and with velocity offsets V_{Z_p} taken randomly in the range $(-V_0, V_0)$. We have taken values of V_0 up to 100 km/s. We recover the 6 phase-space coordinates from $(X, Y, V_Z; Z_p, V_{Z_p})$, i.e. 3 coordinates in the initial system and 2 in the plane system, to which we have added the approximation of orthogonality between the position and velocity vectors.

We find the missing coordinates to be given by:

$$Z = \sec\phi\,(Z_p - (Y\cos\theta + X\sin\theta)\sin\phi), \tag{12}$$

$$V_X = V_{X_p}\cos\theta + \sin\theta\,(V_{Y_p}\cos\phi + V_{Z_p}\sin\phi), \tag{13}$$

$$V_Y = -V_{X_p}\sin\theta + \cos\theta\,(V_{Y_p}\cos\phi + V_{Z_p}\sin\phi), \tag{14}$$

where

$$V_{Y_p} = \frac{V_{Z_p}\cos\phi - V_Z}{\sin\phi},\quad X_p = X\cos\theta - Y\sin\theta, \tag{15}$$

$$Y_p = \sec\phi\,(Y\cos\theta + X\sin\theta - Z_p\sin\phi), \tag{16}$$

$$V_{X_p} = -\frac{Y_p V_{Y_p} + Z_p V_{Z_p}}{X_p}. \tag{17}$$

Then the distance R and velocity V can be derived for each individual galaxy from each set of coordinates.

The three galaxies of the “Near" sub-system are treated separately, since we have shown that they lie in a very thin disk with a high probability (Sec. 7.1). We find for them:

“Near" sub-system: $\langle R_N \rangle = 0.175 \pm 0.018$ Mpc, $\langle V_N \rangle = 259 \pm 15$ km/s.

We have achieved 1000 realizations of the missing coordinates for the 8 identified satellites in the “Far" sub-system, for each values $\sigma_{Z_p} = (0.08,\ 0.14,\ 0.20)$ Mpc and $V_0 = (0, 30, 60)$ km/s. As already noticed, the effect of velocity offsets with respect to a perfect plane remains small, even for an offset as large as ± 100 km/s (see Fig. 14). In each case we have computed the mean values of R and V for each galaxy, then their global mean for the whole “Far" sub-system. We have also considered the effect of velocity measurement errors: they are small and their effect is negligible except for satellite N^o 10 (see Table 1).

From all these simulations we are able to derive the average values of R and V accompanied by a detailed error analysis listing the various contributions to their uncertainty. We find:

"Far" sub-system: $\langle R_F \rangle = 0.88 \pm 0.05 \pm 0.05$ Mpc, $\langle V_F \rangle = 125 \pm 25 \pm 10 \pm 8$ km/s.

The first error comes from the missing coordinates, the second from the uncertainties on the disk properties. The third error on V_F comes from the velocity measurement errors, while the position measurement errors are negligible. Combining all the errors yields $\langle R_F \rangle = 0.88 \pm 0.07$ Mpc and $\langle V_F \rangle = 125 \pm 28$ km/s for the "Far" sub-system. This value of the mean velocity can be compared with the Kepler law expectation for e.g. $GM = 14000 \pm 4000$ Mpc.(km/s)^2 which yields $V_K = \sqrt{GM/R} = 126 \pm 20 \pm 5$ km/s, where the first error comes from hte uncertainty on GM and the second on R_F.

We finally find in every case that, even though we have added missing coordinates randomly chosen in a thick disk (according to our measurement of its thickness $\sigma_{Z_p} = 0.14 \pm 0.06$), the mean values of the 3D distance and velocity R and V remain fully compatible, within their uncertainties, with the Kepler law $V = \sqrt{GM/R}$ issued from the mean "Near" sub-system (see Fig. 14). Moreover, the mean values for the 8 satellites of the "Far" sub-system and their uncertainties in the different configurations considered (red points with error bars in Fig. 14) fully support our previous determination based on the perfect plane approximation (see Figs. 8 and 9), thus supporting also the various results obtained under this approximation.

8. Extension of NGC 5965 environment

Another explanation of the observed configuration of the environmemt of NGC 5965 has been suggested by a referee, namely, that 'the whole phase-space correlation may come from looking into a cosmic filament rather than a bound system'.

In order to test for this possibility, we have extended the research of galaxies around NGC 5965 with the same criteria but now up to a projected distance $r_p = 2$ Mpc. The resulting map for $-350 < V_Z < 350$ km/s (including the new galaxies) is given in Fig. 15. Several arguments go against the filament hypothesis while supporting the satellite hypothesis:

- the new galaxies do not extend beyond $r_p \approx 1.5$ Mpc and have $|V_Z| <\approx 300$ km/s, confirming the isolation of the system, while a filament would be expected to be by far larger and without such a limit;

- all the companions to NGC 5965 are dwarf or small galaxies (except possibly NGC 5971), as expected for the environment of an isolated giant galaxy, while one would expect to see other giant galaxies in a filament. The giant galaxy closest to this system is NGC 5987, which is found to lie at 5.6 Mpc from NGC 5965.

- under the hypothesis of a filament, the radial velocities would be of essentially cosmological nature, allowing to achieve a 3D map of the system. The extension of the system along the line of sight would be ≈ 8.5 Mpc (± 300 km/s for $H_0 = 70$ km/s.Mpc) against $\approx 2.5 \times 1.0$ Mpc in the orthogonal directions. This would result in an unprobable shape (elongated just along the line-of-sight and flattened).

- the new galaxies are distributed along the same direction as the inner system. We have applied the couple method to the extended system. Excluding galaxies N^o 5, 9 and 12 (which have been found to be unbound or cosmological interlopers in our method of constraints, see Appendix A and Fig. 16), we find 58 couples for 19 galaxies. The probability to obtain such a result for a random or non disk-like distribution (which includes the filament case) is $P = 4 \times 10^{-4}$. Then we have applied to the new galaxies the constraint method (Appendix A) and found that two of them cannot be bound. This leads to 57 couples for 17 satellites. The probability to obtain such a configuration in the absence of a disk is $P = 2 \times 10^{-5}$, which definitely excludes the filament hypothesis and strongly supports the existence of a relatively thin disk.

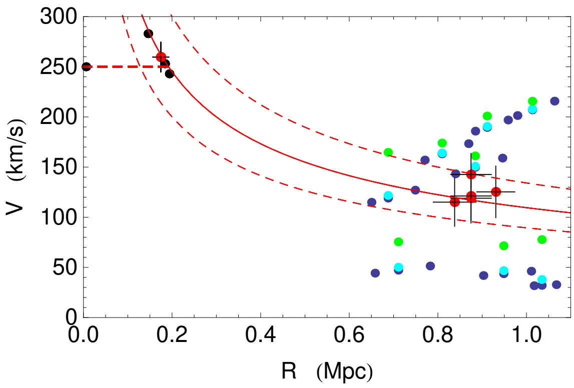

Fig. 14. Mean Kepler law obtained beyond the halo (≈ 200 kpc). For each satellite galaxy, we have plotted the mean (R, V) position for 1000 random realisations of the missing phase-space coordinates. Blue points: $\sigma_{Z_p} = 0.08, 0.14, 0.20$ Mpc, $V_0 = 10$ km/s. Cyan points: $\sigma_{Z_p} = 0.14$ Mpc, $V_0 = 30$ km/s. Green points: $\sigma_{Z_p} = 0.14$ Mpc, $V_0 = 100$ km/s. Red points with error bars: mean of the 8 "Far" galaxies for each configuration. Red curve: Kepler law $V \propto R^{-1/2}$ for $GM = 12000$ Mpc,(km/s)^2. Dashed red curves: Kepler law for $GM = 8000$ and 18000. The horizontal dashed red line stands for an extrapolation of the constant rotation velocity inside NGC 5965 down to ≈ 200 kpc.

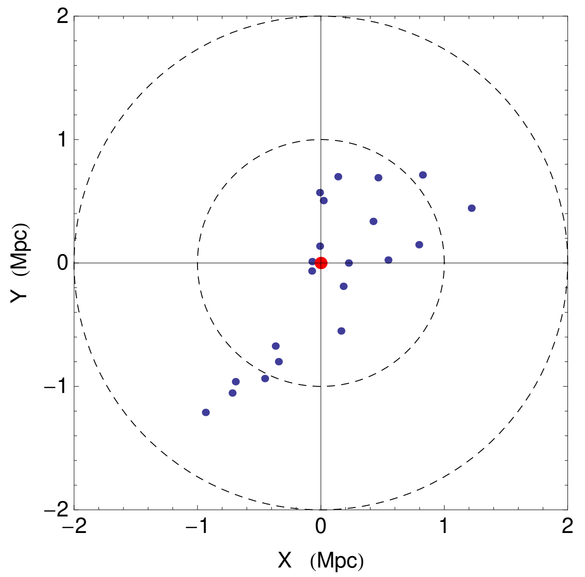

Fig. 15. Distribution on the sky plane of galaxies closer than 2 Mpc from NGC 5965 and velocity difference in the range (−350, 350) km/s.

9. Discussion

In a recent work, Chaves-Montero et al (2021) have identifiied missing baryons from a 11σ detection of the Sunyaev-Zeldovich effect allowing them to set constraints on the location, density, and abundance of gas inducing the SZ effect. They have found that this gas resides outside dark matter haloes, presents densities ranging from 10 to 250 times the cosmic average $\Omega_b = 0.049$, and comprises half of cosmic baryons.

For a r^{-2} halo starting from a mass $10^{11} M_\odot$ at 10 kpc, which would yield a halo mass of $2 \times 10^{12} M_\odot$ at 200 kpc, one finds that this range of density is reached at distances $0.7 - 3$ Mpc, close to the limit 1 Mpc of our satellite catalog. In comparison, at the limit we have found for the halo of NGC 5965, $\approx$ 200 kpc, according to the constant rotation velocity $\approx$ 250 km/s, the density is still $\approx$ 3000 times the mean cosmological baryon density. We conclude that this effect is not expected to perturb our conclusion according to which one recovers Kepler motion in (relative) vacuum beyond $\approx$ 200 kpc.

Remark that the triplet of satellites (2), (3), (4) are compatible with the two laws, constant rotation velocity before their distance to NGC 5965 of about 180 kpc and Kepler law beyond it. There should be a smooth transition between a r^{-2} halo and vacuum around their distance, e.g. with a more rapidly decreasing power law.

Note also that one cannot consider the velocities of this triplet as in continuity with the 'flat rotation curve' of NGC 5965, since its plane and the satellite system plane are different and since we have found no global corotation of the satellites. The constancy is ensured only at the level of the absolute value of the velocities ($\approx$ 250 km/s), not of their orientations, which is sufficient to establish the existence of a non-Newtonian dynamics up to 200 kpc (manifesting an $\approx r^{-2}$ halo in the dark matter hypothesis).

10. Conclusion

In the present paper, we have first constructed an Isolated Galaxy Satellite Catalog (IGSC), in which each host galaxy is alone inside a sphere of 2 Mpc diameter. The host galaxies have been chosen to have absolute magnitudes $M_G < -18.5$ and the difference with satellites to be $\delta M > 2.5$. In other words our isolation criterium is mainly of a gravitational nature. The number of systems in the catalogue is 2931, containing a total of 4849 satellites.

Then we have thoroughly studied one of the members of the IGSC, namely, the system of NGC 5965 and its potential satellites. To this purpose we have conceived a new statistical method based on satellite couples which allows to identify the existence of a disk and to measure its thickness despite the absence of 3 phase-space coordinates among 6. This method has been validated using numrical simulations. Then the main results of our study using this method are the following.

Except for one probable interloper lying at cosmological distance from NGC 5965 which has been excluded and two either out-of-plane or unbound galaxies, the remaining system of 11 satellites has the following characteristics:

- The satellites and their host lie in a disk of relative thickness $\approx 1/7$ (0.14 Mpc / 1 Mpc).

- We confirm the existence of a constant rotation velocity up to $\approx$ 200 kpc basing ourselves on three "Near" satellites and the luminous part of NGC5965. This is, to our knowledge, the first identification of such a non-decreasing rotation velocity for a far galaxy ($V_z = 3383$ km/s) up to such a large distance, which was reached up to now only for our own Milky Way Galaxy and M31.

- Beyond this distance, the velocity profile can be followed thanks to 8 "Far" satellites ($0.6 < r < 1$ Mpc) and it is found to be clearly decreasing. We find that this decrease is fully compatible with a Kepler law from about 200 kpc, up to a large distance $\approx$ 1 Mpc. We have also compared this profile with a NFW ΛCDM model, which predicts a slower decrease, but we have not suceeded fitting the observed velocities at the three available distances ($r_1 \approx 10$ kpc, $r_2 \approx 200$ kpc, $r_3 \approx 800$ kpc) with this model. The MOND hypothesis is also invalidated since the accelerations of these distant galaxies are ≈ 200 times smaller than the MOND limit, while the dynamics is found to remain fully Newtonian.

Acknowledgements: we acknowledge use of the HyperLEDA data base for the construction of the Isolated Galaxy Satellite Catalog. We thank an unknown referee for very helpful suggestions which have allowed us to greatly improve the content of this paper.

Appendix A: constraints on the individual satellite orbital elements

Statement of the problem The questions raised in this Appendix are whether one can distinguish true (bound) satellites from interloper (unbound or cosmological), and to which extent each satellite can be placed in the rather thin disk which has been previously identified in a statistical way (half-thickness 0.14 ± 0.06 Mpc compared to 1 Mpc radius, i.e. axis ratio $\approx 1/7$).

The various possibilities for each satellite are: (1) bound satellite in or close to the main plane; (2) bound satellite out of plane; (3) unbound satellite in hyperbolic orbit; (4) interloper actually at cosmological distance from NGC 5965. We assume, in accordance with our previous results, that the system is Keplerian beyond ≈ 180 kpc, i.e. for all objects except N^o 1A which lies inside or close to the main galaxy (which is subjected to the flat rotation curve) and for one possible (statistically predicted) cosmological interloper.

Global constraints Various constraints can be set on the observed initial coordinates and on the possible mass of the host galaxy. For bound orbits, one expects $R\,V^2 < 2GM$. We have naturally $V \geq V_Z$ and $R \geq \sqrt{X^2+Y^2}$, so that the reconstructed system must be such that:

$$\frac{1}{2}\,V_Z^2 r_P \leq \frac{1}{2}\,V^2 R \leq GM, \tag{18}$$

where $r_P = \sqrt{X^2+Y^2}$ is the projected interdistance. With the available data, one finds the following values for the minimal values $GM_{\min} = \frac{1}{2}\,V_Z^2\,r_P$ in units of Mpc.(km/s)^2:
(sat. N^o, GM_0) = (2, 10), (3, 1083), (4, 1377), (5, 3726), (6, 47), (7, 228), (8, 2194), (9, 11583), (10, 2911), (11, 49), (12, 29363), (13, 5520), (14, 9872), (15, 595).

With $GM = 11600$ we see that all objects can be in bound Keplerian orbits except N^{o}12 which shows the highest departure from the possible limit. This result re-enforces our previous conclusion according to which N^{o}12 is probably an interloper located at cosmological distances from NGC 5965.

Under the perfect plane hypothesis which yields true 3D distances and velocities given by

$$R_0 = \sqrt{x^2 + \frac{y^2}{\cos^2\phi}}, \quad V_0 = |V_z/x|\,\frac{r}{\sin\phi}, \tag{19}$$

another constraint holds, which writes $V_Z < \sqrt{GM/R_0}$. Galaxies N^o 5, 9, and 14 do not satisfy this condition, which implies that they lie out of the plane (but N^{o}14 is relatively close to the plane, see what follows). Galaxies N^o 5 and 9 are most probably unbound objects.

Constraints on missing coordinates Let us now identify the range of possible values of the missing coordinates for each individual galaxy.

For each of the satellites, 3 values of the phase-space coordinates are known, X, Y and V_Z, while 3 are unknown, Z, V_X and V_Y.

In the satellite plane coordinates (index p), the three unknown coordinates can be taken to be Z_p, V_{Xp} and V_{Yp}. Under the assumption according to which both position and velocity vectors lie perfectly in the plane defined by angles θ and ϕ, one has $Z_p = 0$ and $V_{Zp} = 0$, while V_{Xp} and V_{Yp} are given by:

$$V_{Xp} = \frac{V_Z}{\cos\phi\,\sin\phi}\,\frac{y}{x}, \quad V_{Yp} = -\frac{V_Z}{\sin\phi}. \tag{20}$$

Since actually the flatness of the satellite disk is not perfect, there exists offsets from the plane in position and velocity, Z_p and V_{Zp}, which are constrained by the two available relations implementing Newton-Kepler's laws for bound orbits,

$$R\,V^2 = GM\,(1 + e\cos\xi). \tag{21}$$

$$\overrightarrow{R}.\overrightarrow{V} = R\,V\cos\alpha. \tag{22}$$

Here e is the eccentricity of the orbit, $\xi(t)$ the parameter in the parametric representation of the ellipse, $r = a(1 - e\cos\xi)$ and $t = (T/2\pi)(\xi - e\sin\xi)$ and α the angle between the position and velocity vectors. This angle describes the deviation from circularity of orbits. The PDF of α values can be shown to be peaked around $\alpha = \pi/2$ with a narrow width **?**, so that we shall take here the approximation $\cos\alpha = 0$. Only in rare cases one could have a significantly different value: such a possibility will be considered only for the most extreme cases (namely, satellites number 5, 9 and 12). The situation is different as regards $R\,V^2$ which may differ from GM in a significant way. Since we have no access to the time evolution of the orbit, we define $M_\varepsilon = M\,(1+\varepsilon)$ where $-1 < -e < \varepsilon < e < 1$. In other words, M_ε may vary between 0 and $2M$, this upper limit defining the escape velocity $V_{esc} = 2M/R$.

We therefore deal with a system of two equations for three unknown variables, Z_p, V_{Zp} and another velocity, for example V_{Xp}.

We introduce a position offset Z_p from the plane and a possible correction on the radial velocity δV_Z accounting for the measurement error.

The expression for the missing radial coordinate in the original coordinate system can be obtained from the values of Z_p and ε :

$$Z = Z_p \sec\phi - (Y\cos\theta + X\sin\theta)\tan\phi, \tag{23}$$

from which we derive the full distance $R = (X^2 + Y^2 + Z^2)^{1/2}$. Then we set:

$$A_X = -V_Z \frac{Z\cos\theta - Y\cot\phi}{X\cos\theta - Y\sin\theta},\ B_X = \frac{Y\csc\phi}{X\cos\theta - Y\sin\theta}, \tag{24}$$

$$A_Y = V_Z \frac{Z\sin\theta - X\cot\phi}{X\cos\theta - Y\sin\theta},\ B_Y = \frac{X\csc\phi}{X\cos\theta - Y\sin\theta}, \tag{25}$$

$$A_0 = A_X^2 + A_Y^2 + V_Z^2,\ A_1 = A_X B_X + A_Y B_Y,\ A_2 = B_X^2 + B_Y^2. \tag{26}$$

In terms of these quantities and on setting $W = \frac{GM}{R}(1+\varepsilon)$ the velocity offset with respect to the satellite plane has two solutions:

$$V_{Zp} = \frac{-A_1 \pm \sqrt{A_1^2 + A_2(W - A_0)}}{A2}. \tag{27}$$

Finally the two missing velocities write:

$$V_X = A_X + B_X V_{Zp}, \quad V_Y = A_Y + B_Y V_{Zp}. \tag{28}$$

From these results a new constraint emerges in order to get real values for the missing coordinates:

$$A_1^2 + A_2(W - A_0) \geq 0. \tag{29}$$

This constraint is translated into the existence of a limit $\varepsilon_L(Z_p)$ on the quantity ε in the relation $GM(1+\varepsilon) = RV^2$, above which the various calculated coordinates become real while they are imaginary or complex below this curve (red curve in Fig. 16). It is given by:

$$1+\varepsilon_L = \frac{R\,V_Z^2}{GM}\left(1 + \frac{(XZ\cos\theta + YZ\sin\theta - 2XY\cot\phi)^2}{(X\cos\theta - Y\sin\theta)^2\,(X^2+Y^2)}\right), \tag{30}$$

where Z is given in function of Z_p in Eq. 23. The functions $\varepsilon_L(Z_p)$ are shown in Fig. 16 as red curves for the 15 potential satellites.

One can also identify the values of Z_p for which $V_{Zp} = 0$. They are given by the relations $W = A_0$ for one root and ($W = A_0$, $A_1 = 0$) for the other. This is translated into a new curve $\varepsilon_P(Z_p)$ given by:

$$1 + \varepsilon_P = \frac{R\,V_Z^2}{GM}\left(1 + \frac{A^2 + B^2}{(X\cos\theta - Y\sin\theta)^2}\right), \tag{31}$$

where $A = (Z\cos\theta - Y\cot\phi)$ and $B = (Z\sin\theta - X\cot\phi)$. This case therefore corresponds to a velocity vector parallel to the plane. The functions $\varepsilon_P(Z_p)$ are shown as dotted lines for the 15 potential satellites in Fig 16.

The knowledge of the two functions ε_L and ε_P defines the range of possible values for the missing coordinates (see Fig. 16). In particular, it allows one to identify the cases where $Z_p = 0$ is possible. We give in Table 4 an extreme possible reconstruction of the system in which we have minimized the offsets from the plane in position Z_p and in velocity V_{Zp}, while attempting to also keep ε the smallest possible.

We find that $Z_p = 0$ is possible for satellites N° 2, 3, 4, 6, 7, 10, 11, 12, 13, 15, and a small value (−0.05 Mpc) for N° 8. However this is achieved to the price of a high eccentricity (close to 1) for N° 8 and 14, and with an hyperbolic orbit for N° 12, which is therefore unbound or more probably a cosmological interloper. For satellites N° 5, 9 and 14, we find no in-plane solution. However, the angle between the plane and satellite N° 14 radius vector is only -16 deg, which justifies the fact that this satellite was not excluded from the plane in the previous analyses.

After having identified the smallest possible values of Z_p and V_{Zp} for each satellite, we derive the corresponding value of ε, which is given by:

$$\varepsilon = \frac{R}{GM}\,(A_0 + 2A_1 V_{Zp} + A_2 V_{Zp}^2) - 1. \tag{32}$$

The resulting deprojections of the six phase-space coordinates are given in Table 4, with the values of the 3D interdistances and intervelocities and of ε. For this (extreme) reconstruction, we find a disk thickness $\sigma_{Zp} \approx 0.1$ Mpc, which corresponds as could be expected, to a too low value. If instead one favors low values of ε (circular orbits), one finds larger values of Z_p and the thickness becomes ≈ 0.2 Mpc. The effective disk of thickness 0.14 ± 0.06 Mpc clearly stands between these two extremes.

Table 4. Possible example of deprojection of the satellite system around NGC 5965, in which we have favored the smallest possible values of the offset from a perfect plane Z_p (see text). We give the position (in Mpc) and velocity (in km/s) coordinates in the reference system of the mean satellite plane (in which $Z_p = 0$ and $V_{Zp} = 0$), then the 3D distance R and intervelocity V of the satellite with respect to the host galaxy, and finally the parameter $\varepsilon = e \cos \xi$, where e is the excentricity and ξ the orbit parameter in the elliptic case. Bound orbits are characterized by $-1 < \varepsilon < 1$. Object N° 12 has been excluded, being either an interloper or a galaxy unbound to NGC 5965. Bound (elliptical) solutions are still possible for objects N° 5 and 9, but out of plane.

N°	X_p	Y_p	Z_p	V_{Xp}	V_{Yp}	V_{Zp}	R	V	ε
2	-0.015	0.184	0.00	250	23	12	0.184	251	-0.007
3	-0.087	0.117	0.00	-234	-159	6	0.146	283	-0.001
4	0.124	0.149	0.00	-188	158	12	0.194	246	-0.001
5	0.081	0.007	-0.23	63	208	28	0.244	219	0.003
6	-0.111	-0.625	0.00	-132	6	-35	0.635	136	0.011
7	0.48	0.423	0.00	-28	32	-1	0.640	43	-0.900
8	0.466	-0.601	-0.05	-147	-95	6	0.763	175	0.998
9	0.218	-0.222	-0.45	6	195	-68	0.547	206	0.991
10	0.529	0.559	0.00	-121	115	14	0.770	168	0.846
11	-0.455	-0.921	0.00	-29	17	6	1.027	34	-0.899
13	-0.76	0.268	0.00	79	119	-26	0.806	145	0.453
14	0.812	0.119	-0.25	15	-164	6	0.858	165	0.987
15	-0.869	0.087	0.00	-14	47	17	0.873	52	-0.797

References

Anand, G. S., Rizzi, L. & Tully, R. B. 2018, AJ, 156, 105

Bhattacharjee, P., Chaudhury, S., and Kundu S. 2014, ApJ, 785, 63

Bullock, J.S. 2010, Notes on the Missing Satellites Problem, arXiv:1009.4505v1

Burkert, A. 1995, ApJ, 447, L25

Carignan, C., Cote, S., Freeman, K.C. & Quinn, P.J. 1997, AJ, 113, 1585

Chamaraux, P. & Nottale, L. 2016, Astrophys. Bull., 71, 270

Chaves-Montero, J., Hernandez-Monteagudo, C., Angulo, R.E., Emberson, J.D., MNRAS, 503,1798 [arXiv : 1911.10690]

Clowe, D., Bradac, M., Gonzalez A.H., et al. 2006, ApJ 648, L109

Cresson, J., Nottale, L. & Lehner T. 2021, J. Math. Phys. 62, 072702

Dai, D.C, Starkman, G., Stojkovic, D. 2022, Milky Way and M31 rotation curves, arXiv:2201.06034v2

Duc, P.-A., Cuillandre, J.-C., Karabal, E., et al. 2015, MNRAS, 446, 120

Gottesman, S.T., Hunter, J.H. & Shostak, G.S.1983, MNRAS, 212, 21

Gutierrez, C.M. & Azzaro, M. 2004, ApJS, 155, 395

Heesters, N., Habas, R., Marleau, F. R., et al. 2021, A&A, 654, A161

HyperLEDA Database http://leda.univ-lyon1.fr

Ibata, R. A., Lewis, G. F., Conn, A. R., et al. 2013, Nature, 493, 62

Kauffmann, G., White, S. D. M., & Guiderdoni, B. 1993, MNRAS, 264, 201

Klypin, A., Kravtsov, A. V., Valenzuela, O., & Prada, F. 1999, ApJ, 522, 82

Koch, A. & Grebel, E. K. 2006, AJ, 131, 1405

Kuijken and Merrifield, 1995, ApJ443, L13 [arXiv:astro-ph/9501114]

Kunkel, W. E. & Demers, S. 1976, The Galaxy and the Local Group, 182, 241

LeBohec, T. 2022, arXiv:2209.06856

Lynden-Bell, D. 1976, MNRAS, 174, 695

Martinez-Delgado, D., Makarov, D., Javanmardi, B., et al. 2021, A&A, 652, A48

McConnachie, A. W. & Irwin, M. J. 2006, MNRAS, 365, 902

Metz, M., Kroupa, P., & Libeskind, N. I. 2008, ApJ, 680, 287

Milgrom M. 1983, ApJ 270, 365

Moore, B., Ghigna, S., Governato, F., et al. 1999, ApJ, 524, L19

Müller, O., Jerjen, H., & Binggeli, B. 2017, A&A, 597, A7

Müller, O., Rejkuba, M., & Jerjen, H. 2018, A&A, 615, A96

Müller, O., Rejkuba, M., Pawlowski, M.S., et al. 2019, A&A, 629, A18

Müller, O. & Jerjen, H. 2020, A&A, 644, A91

Müller, O., Pawlowski, M. S., Lelli, F., et al. 2021, A&A, 645, L5

Müller, O., Dynamical Masses of Local Group Galaxies, Proceedings of IAU Symposium 379, P. Bonifacio, M.-R. Cioni, F. Hammer, M. Pawlowski, and S. Taibi, eds. [arXiv:2304.13582v1]

Navarro, J. F., Frenk, C. S., & White, S. D. M. 1996, ApJ, 462, 563

Navarro, J. F., Frenk, C. S., & White, S. D. M. 1997, ApJ, 490, 493

ASA/IPAC Extragalactic Data base, https://ned.ipac.caltech.edu/

Nottale L. 2001, in Frontiers of Fundamental Physics, Proceedings of Birla Science Center Fourth International Symposium, 11-13 dec. 2000, Hyderabad, India, Eds. B.G. Sidharth and M.V. Altaisky, (Kluwer Academic), p. 65.

Nottale, L., & Chamaraux P. 2020, A&A 641, A115

Nottale, L., & Chamaraux, P. 2018a, A&A, 614, A45

Nottale, L., & Chamaraux, P. 2018b, Astrophys. Bull., 73, 310

Paudel, S., Yoon, S.J., & Smith R. 2021, ApJ L, 917, L18

Pawlowski, M. S. 2018, Modern Physics Letters A, 33, 1830004

Prada, F., et al. 2003, ApJ, 598, 260

Santos-Santos, I. M., Dominguez-Tenreiro, R., & Pawlowski, M. S. 2020, MNRAS, 499, 3755

Smith, R.M., & Martinez, V. 2003, in ASP Conf. Ser., Satellite Galaxies and Tidal Streams, ed.F. Prada, D. Martinez-Delgado, & T. Mahoney (San Francisco : ASP)

Sofue, Y. 2016, Publ. Astron. Soc. Japan, 68, 2.

Sofue, Y. 2018, Publ. Astron. Soc. Japan, 70, 31.

Tully, R. B., Libeskind, N. I., Karachentsev, I. D., et al. 2015, APJL, 802, L25

Zaritsky, D., Smith, R., Frenk, C., & White, S. 1993, ApJ, 405, 464

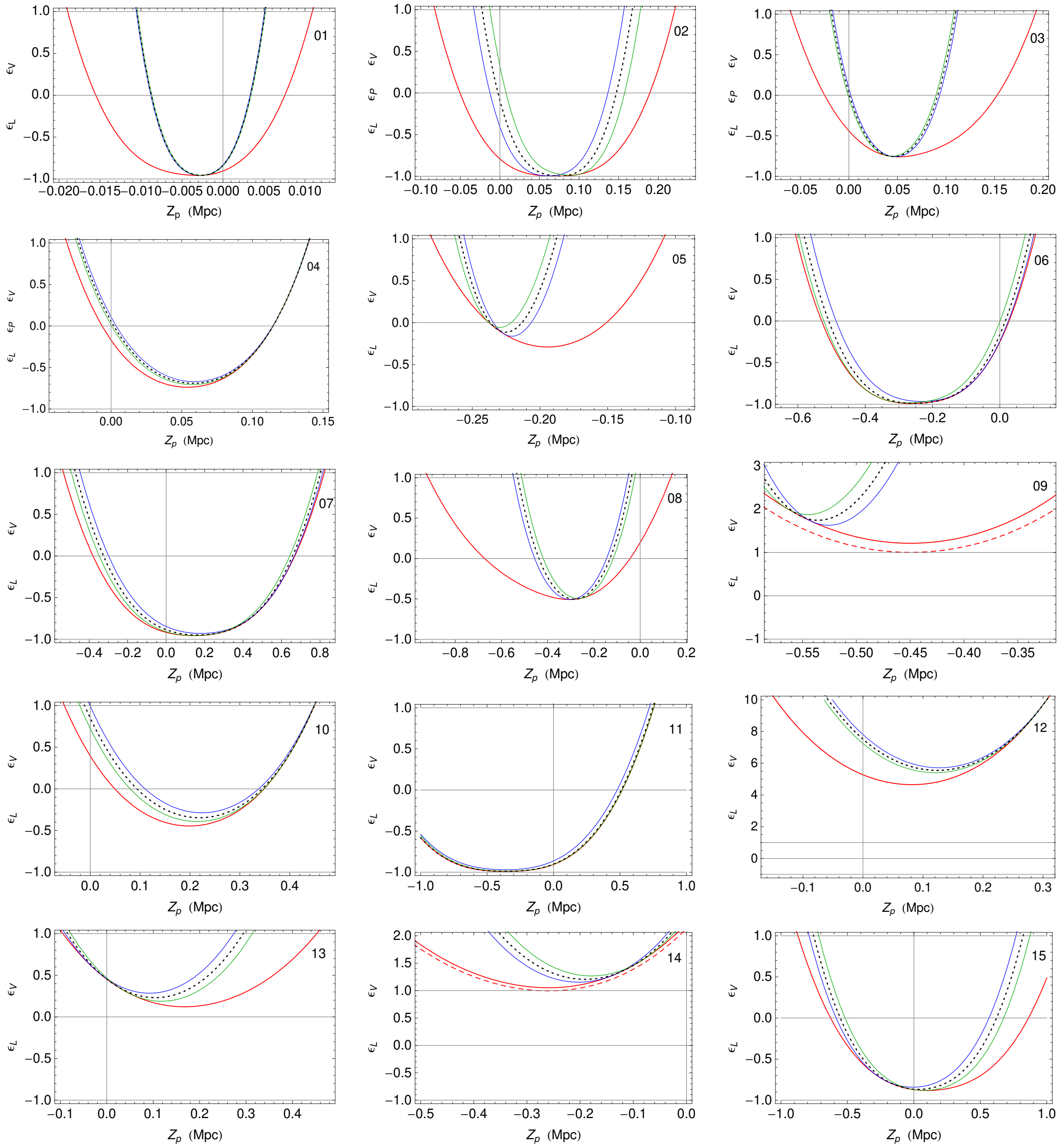

Fig. 16. Diagram (Z_P, ε) for the 15 potential satellites of NGC 5965. The red continuous curve shows the relation $\varepsilon_L(Z_p)$ (Eq. 30) computed for $GM = 10500$. Solutions for the reconstruction of the satellite parameters are possible only above this curve. We have also shown this limit as red dashed curves for satellite N^o 14 with $GM = 10800$ and for satellite N^o 9 with $GM = 11600$. The black dotted curve shows the relation $\varepsilon_P(Z_p)$, which corresponds to no velocity offset from the plane, $V_{Zp} = 0$. The blue curve indicates a velocity offset $V_{Zp} = -10$ km/s and the green curve $V_{Zp} = +10$ km/s. Elliptical (bound) orbits correspond to $-1 < \varepsilon < 1$. Almost all objects can satisfy the conditions of both being bound and in-plane, except N^o 12 which is probably an interloper, and objects N^o 5, 9 and 1) which have no in-plane solution.

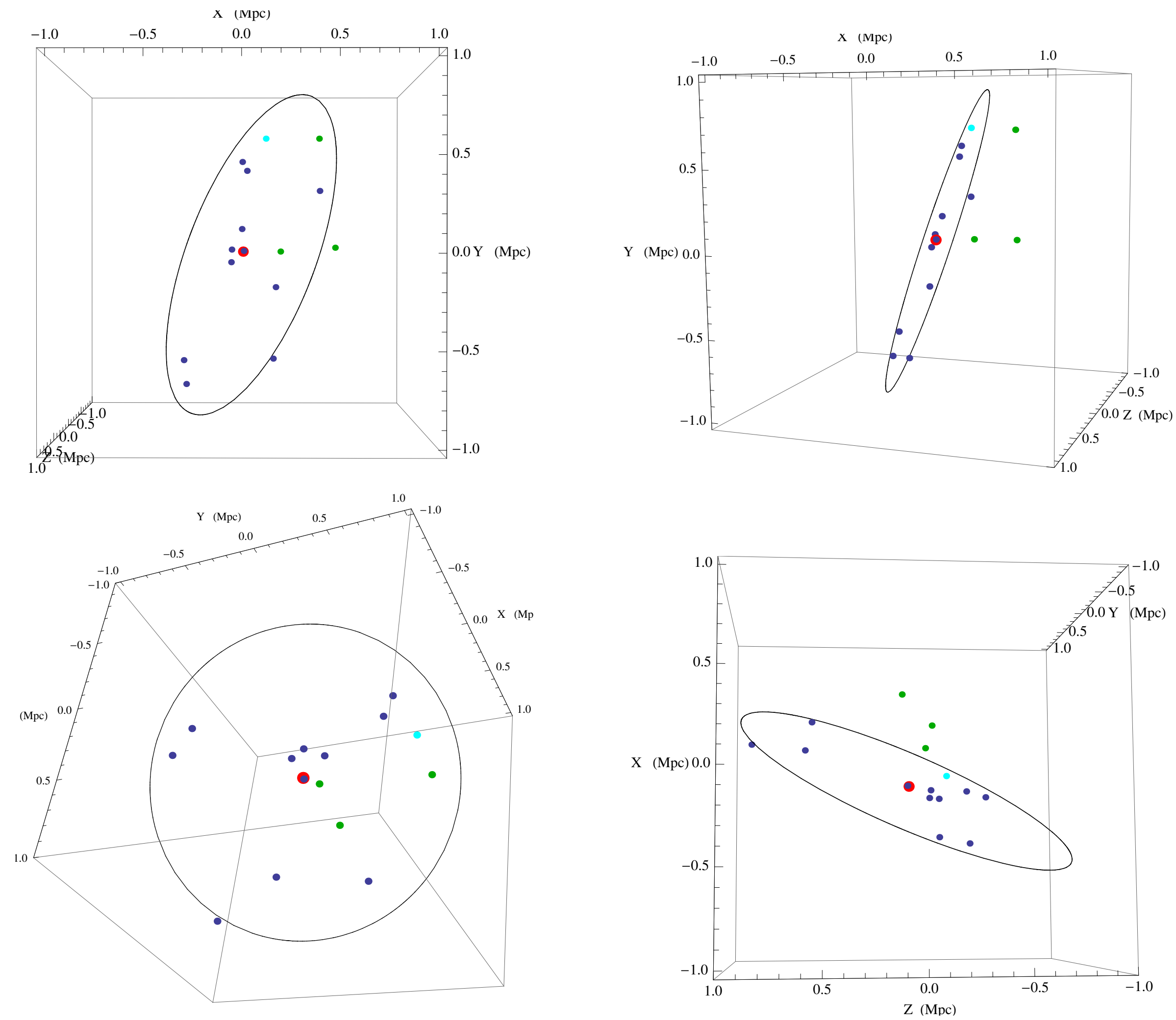

Fig. 17. Views of an example of possible reconstruction of the satellite system around NGC 5965, projected along four different directions. In this (extreme) example, the smallest values of the offset with respect to a perfect plane Z_p have been favored. The red point is NGC 5965. The blue points are in-plane satellites. The cyan point is object N°12 interpreted as an unbound companion crossing the system. Up-left figure: projection on the sky plane (compare with Figs. 2 and 3)). Down-left figure: projection on the satellite plane (compare with Fig. 5). Up-right figure: view projected in a direction close to 90 deg from the satellite plane showing its flattening and the out-of-plane satellites (green points). Down-right figure: another view of the satellite system.